

# EFFECTS OF AN IMPROVED BASELINE AND SELECTION BIAS FOR GROOMED JET DATA IN HEAVY-ION COLLISIONS\*

LILIANA APOLINÁRIO 

LIP, Av. Prof. Gama Pinto 2, 1649-003 Lisboa, Portugal  
and  
Instituto Superior Técnico (IST), Universidade de Lisboa  
Av. Rovisco Pais 1, 1049-001 Lisboa, Portugal

DIOGO COSTA , ALBA SOTO-ONTOSO 

Departamento de Física Teórica y del Cosmos, Universidad de Granada  
Campus de Fuentenueva, 18071 Granada, Spain

*Received 6 April 2026, accepted 28 May 2026,  
published online 10 July 2026*

The plethora of existing jet observables in heavy-ion collisions has allowed for an extensive description of jet quenching phenomena over the last decades. Despite this, we still lack a concise theoretical interpretation of the observed data, namely at the level of jet substructure observables. In an attempt to be dominated by perturbative dynamics, one usually relies on grooming methods which remove soft, wide-angle radiation, but even for this scenario, there are still competing explanations for the physical origin of the measured medium-induced modifications. To this end, we present a minimal approach to compute groomed substructure observables, with medium effects treated as an effective energy shift dependent on the jet substructure itself. By matching the NLO dijet matrix element with a leading-logarithmic-accurate parton shower and using an energy-loss model which includes colour coherence effects, we obtain a solid theory-to-data agreement (within 10%) when compared to ALICE and ATLAS data. We also find an overall better agreement with data when including colour coherence effects and we inspect the role of quark–gluon selection bias.

DOI:10.5506/APhysPolBSupp.19.4-A6

## 1. Introduction

Ultra-relativistic heavy-ion collisions enable us to extensively study the Quark–Gluon Plasma (QGP), a dense QCD medium that behaves as a

---

\* Presented at the Excited QCD 2026 Workshop, Granada, Spain, 8–14 January, 2026.

strongly coupled hot fluid. Due to its short formation time and rapid thermalisation, a direct measurement of its properties is not feasible. Instead, we rely on indirect probes, produced alongside the QGP. Among these, we have jets — collimated sprays of particles originating from the hard scattering. Alongside the jet development, its constituents interact with the QGP resulting in a modification of the jet itself (*e.g.* jet yield suppression, jet substructure modification). These modifications are known as jet quenching and can be used to infer the medium properties.

Inclusive-type measurements (*e.g.* jet yield suppression), which integrate over the complex radiation pattern of jets were essential in the early jet quenching studies. Nevertheless, they quickly became insufficient, as they cannot probe the parton-medium dynamics. Gradually more attention was drawn to jet substructure observables, particularly those employing grooming, which aim at understanding how the medium interacts with different jet structures and with their constituents. From all the vastly new jet substructure data, there was evidence for a strongly quenched jet core with respect to the vacuum baseline.

As of now there is still no clear explanation of the current experimental data due to the coexistence of several mechanisms that are able to quantitatively describe these modifications. In this manuscript, we focus on two of these effects: quark–gluon selection bias and colour-coherence effects. Quark- and gluon-initiated jets are expected to lose energy in the QGP differently due to their distinct fragmentation patterns and overall colour charge. This can modify the effective quark/gluon composition of the reconstructed jet sample and thereby generate an apparent narrowing of groomed jets [1]. Moreover, colour-coherence effects and the finite medium resolution can bias the relative suppression of narrow and wide jets through an angle-dependent pattern of energy loss [2].

Lastly, since jet quenching modifications are estimated based on a theory-to-data comparison between proton–proton ( $pp$ ) and Heavy-Ion (HI) collisions, it is essential to understand what impact a more precise vacuum baseline can have on the interpretation of jet substructure observables. This manuscript shows the main results for one jet substructure observable. For the full jet substructure and baseline corrections analysis, see Ref. [3].

## 2. Bottom-up approach setup

We address this question by implementing a minimal setup based on a bottom-up approach. The idea is to first compute the groomed jets as in vacuum, and *a posteriori*, dress this hard vacuum structure with a radiative energy-loss model, which will essentially shift the jet  $p_T$ . To this end, we build an improved baseline, matching the hard-scattering configuration

with a leading-logarithmic (LL) parton shower. This is done by interfacing POWHEG-BOX [4] with PYTHIA [5]. For the implementation of coherence effects, we use a radiative energy-loss model based on a two-prong antenna configuration and mediated by soft medium-induced gluons in the large-number-of-colours (large- $N_c$ ) approximation [6]. As shown in Ref. [7], this approximation is capable of achieving results with deviations of up to 1%

$$P_2^R(\varepsilon, \theta_{12}, L) = \int_0^\infty d\varepsilon_1 \int_0^\infty d\varepsilon_2 P_1^R(\varepsilon_1, L) P_{\text{sing}}(\varepsilon_2, \theta_{12}, L) \delta(\varepsilon - \varepsilon_1 - \varepsilon_2), \quad (1)$$

with  $\theta_{12}$  the dipole opening angle and  $R$  the parent colour charge. Moreover,  $P_1^R$  is the energy loss distribution of a single parton and is given by

$$P_1^R(\varepsilon, L) = \sqrt{2 \frac{\omega_s^R}{\varepsilon^3}} \exp \left[ -2\pi \frac{\omega_s^R}{\varepsilon} \right], \quad \omega_s^R = \frac{\alpha_{\text{s,med}}^2 C_R^2}{2\pi^2} \hat{q} L^2, \quad (2)$$

where  $C_R = C_A = 3$  for gluon-initiated splittings and  $C_R = C_F = C_A/2$  for quark-initiated splittings (using the large- $N_c$  limit). Lastly, the  $P_{\text{sing}}$  term in Eq. (1) describes the energy loss of a colour-singlet dipole and reads

$$P_{\text{sing}}(\varepsilon, \theta_{12}, L) = P_1^A(\varepsilon, L) - \int_0^L dt P_1^A(\varepsilon, L-t) F(\varepsilon, L-t) [1 - \Delta_{\text{med}}(t, \theta_{12})], \quad (3)$$

with  $F(\varepsilon, L-t) = 1/(L-t) - 4\pi\omega_r^A(L-t)/\varepsilon$ ,  $\omega_r^A = \omega_s^A/L^2$ , and  $\Delta_{\text{med}}(t, \theta_{12}) = 1 - \exp[-\hat{q}\theta_{12}^2 t^3/12]$ , the latter is also known as the decoherence parameter. From  $\Delta_{\text{med}}$ , one can define a critical angle  $\theta_c \sim (\hat{q}L^3)^{-1/2}$ . For  $\theta_{12} \gg \theta_c$ , we are said to be in the incoherent regime, the medium is able to resolve both branches independently, and the antenna loses energy as two colour charges. On the other hand, for  $\theta_{12} \ll \theta_c$  we are said to be in the coherent regime and the antenna is resolved as a single colour structure given by the mother colour charge. In order to disentangle from colour coherence effects and the selection bias, we compared the quenched groomed jet observables computed for both the  $P_1^R(\varepsilon, L)$  and  $P_2^R(\varepsilon, \theta_{12}, L)$  energy-loss models.

### 3. Bottom-up approach results

We show in Fig. 1 the results obtained with this improved baseline when compared to recent ALICE [8] and ATLAS [9] data. To recover the antenna-type structure of Eq. (1), we started by clustering the event using the anti- $k_T$  algorithm with a jet radius  $R$  and afterwards reclustered these jets with the Cambridge/Aachen algorithm. Lastly, the SoftDrop

(SD) grooming algorithm [10] was applied to these reclustered jets. The computed pair of subjets  $j_1$  and  $j_2$ , which satisfy the SD condition was then identified as the antenna to be further quenched. One should mention that, for this manuscript, we will only focus on one of the analysed groomed jet substructure observables, the groomed opening angle  $\theta_g = r_g/R$ , with  $r_g = \sqrt{(y_{j_1} - y_{j_2})^2 + (\phi_{j_1} - \phi_{j_2})^2}$ .

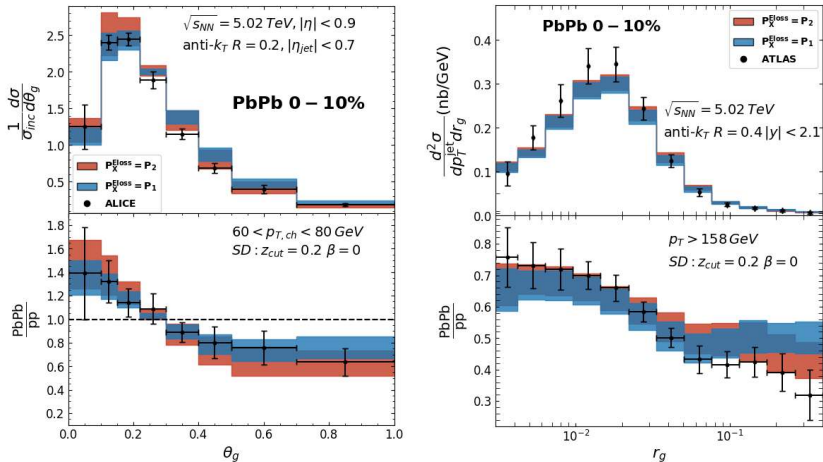


Fig. 1. (Colour on-line) PbPb  $\theta_g$  distribution obtained using POWHEG+PYTHIA 8 and both energy-loss models:  $P_2^R$  (red), in Eq. (1) and  $P_1^R$  (blue), in Eq. (2). Left: comparison to ALICE data, Right: comparison to ATLAS data. The band in the simulation results corresponds to the combination of the standard deviation with the  $\hat{q}$  uncertainty.

Starting with the ALICE comparison, given in the left plot, there is an overall quantitative agreement with data, both for the full distributions and the PbPb–pp ratios. For  $P_2^R$ , we notice a greater suppression for larger  $\theta_g$  values when compared to  $P_1^R$ . This is to be expected, since at larger angles, specifically for  $\theta_g \gg \theta_c$ ,  $P_2^R$  will effectively correspond to an independent two-prong energy loss. Despite these differences between energy-loss models, there is still an agreement with data when using  $P_1^R$ , indicating that current experimental uncertainty does not yet allow one to discriminate between the two scenarios. Focusing now on the ATLAS results, given in the right plot, there is still an overall quantitative agreement with data when using  $P_2^R$ . Nevertheless, for these fiducial cuts, deviations start to appear for higher  $\theta_g$  values when using  $P_1^R$ . Given the current statistical significance, it is not possible to claim the existence of coherence effects. That said, this indicates that these observables might point in the right direction for further evidence.

#### 4. Selection bias

To better understand the influence on the selection bias, we explored its impact in a simplified fixed-order scenario. We generated the hard scattering using MADGRAPH [11] and clustered the event using the same procedure as previously, the difference being that we now only considered two parton jets that satisfy the SD condition. In Fig. 2 (left), we show the self-normalised in-medium  $\theta_g$  distribution for different  $\hat{q}$  values obtained using  $P_2^R$ . Even for this simplified scenario, one can already obtain the trend seen in data. Although not shown, when using  $P_1^R$ , we obtained a flat PbPb– $pp$  ratio. To understand this result, we show in Fig. 2 (right) the vacuum and in-medium  $\theta_g$  distributions per jet initiator. Even though the jet sample is an admixture of quark- and gluon-initiated jets, there seems to be no correlation with the distribution shape. This explains why there is no narrowing effect while still having an increase in the in-medium quark fraction. This calculation was repeated when considering the parton shower, and for this case, the distribution shape clearly depends on the initiating particle, explaining the existence of a narrowing effect for full events.

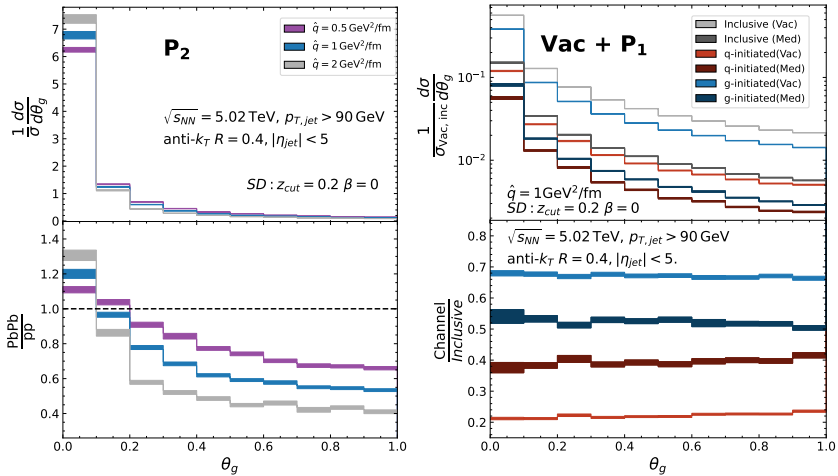


Fig. 2. Left: Self-normalized PbPb  $\theta_g$  distribution for different values of  $\hat{q}$ . Right:  $pp$  and PbPb  $\theta_g$  distributions for different channels. The vacuum cross section was computed using MADGRAPH, and the energy-loss distribution used was  $P_2^R$ , Eq. (1) for the left plot, and  $P_1^R$ , Eq. (2), for the right plot. The error band in each line represents an uncertainty estimate as provided by MADGRAPH.

## 5. Summary and outlook

We have shown, in this manuscript, a minimal bottom-up approach to study groomed jet observables in heavy-ion collisions. We improved the standard baseline accuracy by using an NLO+LL baseline. When embedding this improved baseline with a coherence-based energy-loss model, we find very good theory-to-data agreement for recent ALICE and ATLAS data (within 10%). Despite its simplicity and current statistical significance, we look forward to more formal statistical use of this model, as well as for future, more precise experimental data expected from the upcoming LHC Run 4.

D.C. has been supported by MCIN/AEI (10.13039/501100011033) and ERDF (grant PID2022-139466NB-C21), by the Consejería de Universidad, Investigación e Innovación, Gobierno de España, and Unión Europea — NextGenerationEU, under grant AST22 6.5, and by the Ramón y Cajal program under grant RYC2022-037846-I. A.S.O. is supported by the Ramón y Cajal program under grant RYC2022-037846-I and by ERDF (grant PID2024-161668NB-100). This work is also supported by the Fundação para a Ciência e a Tecnologia (FCT), under ERC-PT A-Projects ‘Unveiling’, financed by PRR, NextGenerationEU. L.A. acknowledges support from FCT under contract 2021.03209.CEECIND.

## REFERENCES

- [1] M. Spousta, B. Cole, *Eur. Phys. J. C* **76**, 50 (2016).
- [2] Y. Mehtar-Tani, C.A. Salgado, K. Tywoniuk, *Phys. Rev. Lett.* **106**, 122002 (2011).
- [3] L. Apolinário, D. Costa, A. Soto-Ontoso, [arXiv:2601.13310 \[hep-ph\]](https://arxiv.org/abs/2601.13310).
- [4] P. Nason, *J. High Energy Phys.* **2004**, 040 (2004).
- [5] C. Bierlich *et al.*, *SciPost Phys. Codeb.* **2022**, 8 (2022).
- [6] Y. Mehtar-Tani, K. Tywoniuk, *Nucl. Phys. A* **979**, 165 (2018).
- [7] J.H. Isaksen, K. Tywoniuk, *J. High Energy Phys.* **2023**, 049 (2023).
- [8] Large Ion Collider Experiment and ALICE Collaboration (S. Acharya *et al.*), *Phys. Rev. Lett.* **128**, 102001 (2022).
- [9] ATLAS Collaboration (G. Aad *et al.*), *Phys. Rev. C* **107**, 054909 (2023).
- [10] A.J. Larkoski, S. Marzani, G. Soyez, J. Thaler, *J. High Energy Phys.* **2014**, 146 (2014).
- [11] J. Alwall *et al.*, *J. High Energy Phys.* **2014**, 079 (2014).